

ORIGINAL ARTICLE

Loss-of-function or gain-of-function variations in *VINCULIN* (*VCL*) are risk factors of human neural tube defects

Yalan Wang¹  | Yue Qin² | Rui Peng¹ | Hongyan Wang^{1,2,3,4}

¹Obstetrics & Gynecology Hospital, Institute of Reproduction & Development, Fudan University, Shanghai, China

²State Key Laboratory of Genetic, Engineering at School of Life Sciences, Fudan University, Shanghai, China

³Key Laboratory of Reproduction Regulation of NPFC, Collaborative Innovation Center of Genetics and Development, Fudan University, Shanghai, China

⁴Collaborative Innovation Center for Genetics and Development, School of Life Sciences, Fudan University, Shanghai, China

Correspondence

Hongyan Wang, Obstetrics & Gynecology Hospital, Institute of Reproduction & Development, Fudan University, Shanghai 200001, China.
Email: wanghy@fudan.edu.cn

Funding information

National Natural Science Foundation of China, Grant/Award Number: 31771669; National Key Research and Development Program of China, Grant/Award Number: 2016YFC1000502

Abstract

Background: Neural tube defects (NTDs) are severe birth defects resulting from the failure of neural tube closure during embryogenesis. Both genetic and environmental factors contribute to the occurrence of NTDs and the heritability of NTDs is approximately 70%. As a key component of focal adhesions, Vinculin (*VCL*) plays pivotal roles in cell skeleton remodeling and signal transduction. *Vcl* deficient mice displayed NTD, but how *VCL* variants contribute to human NTDs has not been addressed yet.

Methods: We screened *VCL* variants in a Chinese cohort of 387 NTDs and 244 controls by targeted next-generation sequencing.

Results: We identified four case-specific *VCL* variations (p.M209L, p.D256fs, p.L555V and p.R586Q). *VCL* p.D256fs and p.L555V are novel variations that have never been reported. Our analysis revealed that p.D256fs is a loss-of-function variant, while p.L555V showed a gain of function in planner cell polarity (PCP) pathway regulation and cell migration, probably due to its enhanced protein stability.

Conclusion: Our study reports human NTD specific novel variations in *VCL* and provides the functional evaluation of *VCL* variants related to the etiology of human NTDs.

KEY WORDS

neural tube defect, PCP signaling, variant, *VCL*

1 | INTRODUCTION

Neural tube defects (NTDs), a common class of severe birth defects, accounting for 0.5 to 2 per 1000 established pregnancies in different regions (Copp et al., 2013). The neural tube is developed through a series of processes, including shape, bend, and fuse of the neural plate and eventually form of the complete neural tube in high vertebrates (Greene & Copp, 2014). NTDs result from the failure of the neural tube closure (NTC) which happens during the

third and fourth weeks of gestation in humans. According to the malformation position, NTDs can be classified into five subtypes, including exencephaly, anencephaly, craniorachischisis, myelomeningocele (spina bifida), and encephalocele (Copp et al., 2013). Both genetic and environmental factors are implicated in the pathogenesis of NTDs, and not more than 70% of NTDs occurrence can be explained by genetic variants (Leck, 1974). More than 200 genes have been reported to be causative for the NTD phenotype in mice (Harris & Juriloff, 2010), providing

This is an open access article under the terms of the Creative Commons Attribution-NonCommercial-NoDerivs License, which permits use and distribution in any medium, provided the original work is properly cited, the use is non-commercial and no modifications or adaptations are made.

© 2021 The Authors. *Molecular Genetics & Genomic Medicine* published by Wiley Periodicals LLC.

hundreds of candidate genes for human NTDs. However, only a few candidate genes, such as *VANGL1*, *VANGL2*, *CELSR1*, have been confirmed to be mutated and contribute in/to human NTDs (Murdoch et al., 2014). Previous studies have revealed that a variety of signaling pathways, such as planar cell polarity (PCP; Lei et al., 2010; Murdoch et al., 2014), sonic hedgehog (SHH; Murdoch & Copp, 2010; Ybot-Gonzalez et al., 2002), and bone morphogenetic protein (BMP; Ybot-Gonzalez et al., 2002, 2007), are implicated in human NTDs (Au et al., 2010). Notably, PCP is the most intensively studied pathway in deciphering the etiology of human NTD and variations in NTD-related PCP genes, such as *VANGL1* (Kibar et al., 2007), *VANGL2* (Lei et al., 2010), *FZD6* (De Marco et al., 2012), *LRP6* (Lei et al., 2015), *SCRIB* (Lei et al., 2013), *DVL2* (De Marco et al., 2013), was gradually identified.

Vinculin (VCL) is a key component of focal adhesions (FAs) involved in cell skeleton remodeling and signal transduction during development and homeostasis (Atherton et al., 2015). The primary structure of VCL consists of the globular head domain, a tail domain, and an in-between proline-rich region (JM & AS, 2013). There is a wide range of binding partners for VCL, and the binding is modulated by the intramolecular auto-inhibitory interaction between its head and tail (Case et al., 2015; RP & SW, 1995). VCL transformation from auto-inhibition to the activation state is spatio-temporally regulated in FAs (Case et al., 2015). Active VCL can positively reinforce FAs (Case et al., 2015), which is essential for FAs-mediated tissue morphogenesis. VCL plays important roles in the maintenance of cell polarity and migration, which is fundamental in embryonic development including neural tube closure. Expression of active vinculin attenuates cell polarity and migration (Carisey et al., 2013), while the loss of VCL leads to increased cell migration (Chinthalapudi et al., 2014; Lausecker et al., 2018; Xu et al., 1998). *Vcl* knockout mice died around E8 to E10 with a series of NTD phenotypes including lacking of the midline fusion of the rostral neural tube, a cranial bilobular appearance, and attenuation of cranial and spinal nerve development in addition to severe defects of heart development (Xu et al., 1998). Although VCL mutations were associated with human hypertrophic or dilated cardiomyopathy (Vasile et al., 2006; Vasile, Will, et al., 2006), whether VCL variants contribute to human NTDs remains elusive. To address whether VCL is implicated in the pathogenesis of human NTDs, we conducted the next-generation targeted sequencing of VCL exons in 387 NTD samples and 244 healthy controls. Four case-specific variants (*VCL* p.M209L, *VCL* p.D256fs, *VCL* p.L555V and *VCL* p.R586Q) were identified and the functional impacts of these variants on VCL protein were assessed by biological assays. Loss-of-function variant *VCL* p.D256fs and gain-of-function variant *VCL* p.L555V were considered as risk factors for human NTD.

TABLE 1 Demographic characteristics in NTD cases and controls.

Variable	Case	Control
Sequence group	387	224
Region		
Tianjin	47	0
Jiangsu	25	0
Liaoning	29	0
Heilongjiang	16	0
Shanxi	270	192
Shanghai	0	32
Age: weeks/years (mean ± SD)		
Tianjin	N.D.	
Jiangsu	N.D.	
Liaoning	25.2 ± 40.8 m	
Heilongjiang	N.D.	
Shanxi	23.4 ± 6.2 w	20.0 ± 3.2 w
Shanghai		18.0 y
Gender		
Male	41.1%	40.6%
Female	30.7%	58.9%
Unknown	28.2%	0.5%
NTD classification		
Craniorachischisis	19	
Encephalocele	76	
Anencephaly	77	
Exencephaly	1	
Spina bifida	167	
Other ^a	47	

^aMore than one kind of NTD phenotype.

2 | MATERIALS AND METHODS

2.1 | Ethical Compliance

This study was approved by the Ethics Committee of the School of Life Sciences, Fudan University, and conducted following the Declaration of Helsinki principles. All of these samples were collected with informed parental consent.

2.2 | Study subjects

Subjects participated were recruited from 2008 to 2014 and all ethnic Han Chinese, including 387 patients or aborted fetuses with NTDs and 244 blood from healthy controls or tissue samples from aborted fetuses without NTDs. NTD samples (41.1% male, 30.7% female, 28.3% unknown) were collected from Tianjin (47), Jiangsu (25), Liaoning (29), Heilongjiang (16), Shanxi (270) in China (Table 1).

All NTD samples were classified into Craniorachischisis, Encephalocele, Anencephaly, Exencephaly, Spina bifida or others (with more than one type of NTD symptoms). The 224 controls (40.6% male, 58.9% female, 0.45% unknown) were recruited from Shanxi (192 tissue samples from aborted healthy fetuses) or Shanghai (32 blood samples from healthy freshmen) in China (Table 1).

2.3 | DNA sequencing, genotyping, and data analysis

Approximately 2 ml of peripheral blood or 50 µg of tissue samples was collected for genomic DNA extraction. The coding regions in *VCL* were amplified by PCR and sequenced by targeted next-generation sequencing as previously described (Qiao et al., 2016), and then compared with the human *VCL* cDNA (NM_003373.3) in the GenBank database. To confirm the *VCL* variants from next-generation sequencing, ~500 bp fragments of the *VCL* gene flanked each variation sites were generated by PCR and re-sequenced by Sanger sequencing (Sangon, China). Primers used are listed in Table S1. SIFT (<http://sift.jcvi.org/>) and Mutation Taster2 (<http://www.mutat iontaster.org/>) were used to predict the impact consequences of missense variants. *VCL* variants were searched in two public databases: the 1000 genome project (<http://www.1000g enomes.org>) and the The Genome Aggregation Database (gnomAD; <http://gnomad.broadinstitute.org/>).

2.4 | Plasmid construction

The human *VCL* (NM_003373) cDNA clone was purchased from OriGene Technologies (Beijing, China) and inserted into the mammalian expressing plasmid pCMV6-AN-DDK. All variants of *VCL* were generated using a QuikChange Site-Directed Mutagenesis Kit (TOYOBO, Japan). Primers used for plasmids construction are listed in Table S1. All plasmids were confirmed by sequencing.

2.5 | Western blot

N-terminal Flag-tagged *VCL* expressing plasmids were co-transfected into HEK293T cells together with pCMV6-AC-GFP as transfection control. Thirty-six hours posttransfection, cells were further treated without/with MG132 for 12 hr and then collected/lysed with lysis buffer [150 mM of NaCl, 50 mM of Tris (pH7.4), 1% NP-40, 0.25% sodium deoxycholate, 1×Cocktail protease inhibitors (Roche, 04693116001)]. The cell lysates were separated by 10% SDS-PAGE and then transferred to PVDF membranes (Millipore). After blocking with 5% nonfat milk, the membranes were incubated with

the anti-Flag antibody (CST, 8146S) or anti-GFP antibody (OriGene, TA150041) at 4 °C overnight. Protein bands were visualized by chemiluminescence using ECL Western Blotting Substrate (Tanon, 180–501) after incubating with secondary antibody. Three independent experiments were performed and the band intensity was quantitatively measured by ImageJ software.

2.6 | RNA isolation and qRT-PCR

HEK293T cells transfected with empty vector, wild-type or variant *VCL* plasmids were collected at 24 hr after transfection. RNA simple Total RNA Kit (TIANGEN; DP419) was used for RNA extraction, and then cDNA reverse transcription was performed using the FastQuant RT kit (TIANGEN; KR106). Q-RT-PCR was carried out on CFX96 (Bio-Rad) using Super Real PreMix SYBR Green (TIANGEN; FP205). *VCL* mRNA levels were normalized by *GAPDH*. Primers used for qRT-PCR are listed in Table S1. Three independent experiments were performed and each group was analyzed in triplicate.

2.7 | Immunofluorescence staining

The HEK293T cells were seeded on coverslip slides (WHB, WHB-12-cs) coated by Polylysine (Sigma, P-9155) inside the 12-well plate and transfected with wild-type or variant *VCL* expressing plasmids. Twenty-four hours posttransfection, cells were rinsed in PBS, followed by 4% PFA for 30 min. After that, the cells were permeabilized with 0.3% TritonX-100 and blocked with 5% Donkey serum (Solarbio, SL050). Next, the cells were sequentially incubated with anti-Flag antibody (CST, 8146S) at 4 °C overnight and FITC conjugated anti-mouse secondary antibody (Abcam, ab6785) for 1 hr at room temperature. The cells were stained with DAPI for 10 min, and then images were obtained with a fluorescence confocal microscope (Zeiss, D710). Three independent experiments were performed.

2.8 | Luciferase reporter assay

The HEK293T cells were seeded on 24-well plates. Empty vector or various *VCL* expressing plasmids, together with Pfa2-c-Jun and JNK-responsive pFR-luciferase plasmids, were transfected with Lipofectamine 2000 (Life Technologies, 11668019). Before being collected, cells were treated with 100 ng/ml of Wnt5A (R&D, 645-WN-010) or vehicle alone for 8 hr and then lysed with 1×Passive lysis buffer (Promega, E1910). The luciferase enzyme activities were analyzed with Dual Luciferase Assay kit (Promega,

TABLE 2 Nonsynonymous NTD case-specific variants within the VCL coding region found in the cohort.

Nucleotide change ^a	aa. change ^b	SIFT	Mutation Taster2	Number in Case (387)	Number in Control (224)	dbSNP	MAF 1000G freq	MAF in gnomAD
c.625A>T	p.M209L	0.28 Tolerated	disease causing	1	0	rs144683137	2×10^{-4}	3.6×10^{-5}
c.768delT	p.D256fs	NA ^c	disease causing	1	0	NA	NA	NA
c.1663C>G	p.L555V	0.008 Damaging	disease causing	1	0	NA	NA	NA
c.1757G>A	p.R586Q	0.57 Tolerated	probably harmless	2	0	rs774076269	NA	8.0×10^{-6}

^aFor nucleotide numbering, +1 corresponds to the A of ATG of mRNA sequence NM_003373.3.

^bReference protein sequence NP_003364.1.

^cNot available.

E1960) according to the manufacturer's instructions. Firefly luciferase activities were normalized with Renilla luciferase control. Three independent transfection experiments were performed, and each luciferase assay was carried out in triplicate.

2.9 | Wound healing assay

H1299 cell was seeded in the 6-well plate and transfected with empty vector or various *VCL* expressing plasmids. Sixteen-hours posttransfection, the cells were scraped by yellow pipet tips. Cell debris was washed away with PBS, and then 2 ml of fresh media was replenished (DMEM with 10% FBS) in each well. The wounds were imaged by an optical microscope at 0 and 16 hr later. Three independent experiments were performed for quantitative measures by ImageJ software.

2.10 | Statistical analysis

Student's *t*-test was used to compare the difference between groups. Statistical analysis was performed with the SPSS software and the data are presented as mean \pm SD ($*p < 0.05$ and $**p < 0.01$).

3 | RESULTS

3.1 | Case-specific *VCL* variants were identified in a cohort of Chinese NTDs

To explore the role of *VCL* in human NTD, we sequenced all exons of *VCL* in a Chinese NTD cohort with 387 cases and 224 controls (Table 1). Compared with controls, three *VCL* single-nucleotide variants (SNVs) including c.625A>T p.M209L, c.1663C>G p.L555V, and c.1757G>A p.R586Q (thereafter called p.M209L, p.L555V, p.R586Q, respectively) and one *VCL* frame-shift variant c.768delT p.D256Efs*9 (thereafter called p.D256fs) were identified as case-specific variants (Table 2). Filtered with databases of Genome 1000 and gnomAD, variants p.D256fs and p.L555V have never been reported, which means that both p.D256fs and p.L555V are novel and rare variants (Table 2). The occurring frequency of p.M209L and p.R586Q were 3.6×10^{-5} and 8.0×10^{-6} , respectively, in the gnomAD database. Variant p.L555V was predicted to be damaging or disease-causing by SIFT and Mutation Taster2, while variants p.M209L and p.R586Q were inconsistently evaluated to be tolerated or detrimental. Frame-shift variant p.D256fs was predicted as disease-causing by Mutation Taster2 (Table 2).

All of the case-specific variations locate at the head domain of VCL and are heterozygous (Figure 1a,b). These four variations were identified from five different samples and p.R586Q variation was recurrently detected in two unrelated NTD samples (Figure 1b). The p.D256fs variation was identified from a 3.5-month-old male patient diagnosed with meningocele, while the three other VCL SNVs were found in four aborted fetuses carrying quite different NTD symptoms, including anencephaly, opened spinal dysraphism, Occipital encephalocele (Table 3). Amino acids D256 and L555 of the VCL protein are highly conserved among different vertebrate species (Figure 1c). Particularly, the five NTD cases with each of the aforementioned case-specific variants did not combinedly carry other NTD-associated mutations in PCP genes such as *VANGLI1*, *VANGL2*, *LRP6*, *SCRIB*, *DVL1-3* and *CELSRI-3*, which helps us to exclude the possibility of a pre-existed effect on PCP signaling.

3.2 | VCL variants affect protein level but not the subcellular localization

Before exploring the functional effects of the VCL variations, the protein level and subcellular localization of each variant were examined. Although the same dose of plasmids was transfected into cells, all variants except for p.M209L showed altered protein levels compared with wild-type VCL. Overexpressed p.D256fs showed no detectable protein and even no truncated protein, even though p.D256fs would undergo a premature termination at translation level and was predicted to produce a short peptide with 265 amino acids (Figure 2a). Although the corresponding mRNA level was not changed, both p.L555V and p.R586Q variants showed higher protein level (Figure 2a,b). This result indicates that the p.L555V and p.R586Q variants might affect protein stability. In order to test this possibility, we treated the cells with MG-132, a proteasome inhibitor, to prevent protein degradation. Interestingly, after MG132 treatment, two variants (p.L555V and p.R586Q) and wide type VCL displayed comparable protein levels, suggesting that the wide-type VCL protein is less

stable than p.L555V and p.R586Q variants proteins. So we speculate that the enhanced protein level of variants p.L555V and p.R586Q might be attributed to the improved protein stability (Figure 2c). In addition, the subcellular localization of WT and variants were also determined by immunofluorescence staining. p.D256fs showed undetectable signal, while the three other variants showed similar distribution patterns with wide type, mainly locating in the cytoplasm (Figure 2d).

3.3 | VCL p.L555V variant affect PCP signaling and cell migration through gain of function

Cytoskeleton remodeling is fundamental and essential for protrusion formation and cell polarity during convergent extension in NTC (Nikolopoulou et al., 2017). The diverse signaling pathways regulating cytoskeleton remodeling are coordinated by focal adhesion. By binding to Talin, VCL maintains integrins in an active conformation and stabilizes the entire FA structure which contains a large number of signaling components (Atherton et al., 2015). We and others found that mutations of PCP pathway components caused NTDs in humans (Kibar et al., 2007; Lei et al., 2010). It is intriguing to test whether VCL plays a regulatory role in the PCP pathway. Dual-luciferase reporter assay indicated that wide-type VCL inhibited basic PCP signaling, but enhanced Wnt5A-activated PCP signaling (Figure 3a). Compared with wide type, p.L555V enhanced the Wnt5A-activated PCP signaling but no effect on basic PCP signaling, while p.M209L and p.R586Q had no effects on both basic and Wnt5A-activated PCP signaling. These results suggest that VCL functions as a negative regulator of basic PCP signaling and potentiates the Wnt5A-activated PCP signaling. In consistency with the protein level (Figure 2a), p.L555V served as a gain-of-function variant on Wnt5A-activated PCP signaling.

During the NTC process, cell movement is propelled by a highly polarized cell shape with protrusions and adhesions (Morita et al., 2012). Although VCL has been proved to coordinate cell migration (Chinthalapudi et al., 2014; Lausacker

TABLE 3 Genotype and phenotypes of cases carrying the case-specific rare variations in VCL.

Variation	Sample	Age (weeks/months ^a)	Sex	Clinical symptoms
p.M209L	D140	23 W	F	Anencephaly, opened spinal dysraphism
p.D256fs	SY425	3.5 M	M	meningocele
p.L555V	D30	16 W	F	Anencephaly
p.R586Q	D62	21 W	M	Occipital encephalocele, Hydrocephalus
	D36	26 W	F	Opened spinal dysraphism, Hydrocephalus

^aWeeks mean the gestation period, while months stand for the postnatal stage.

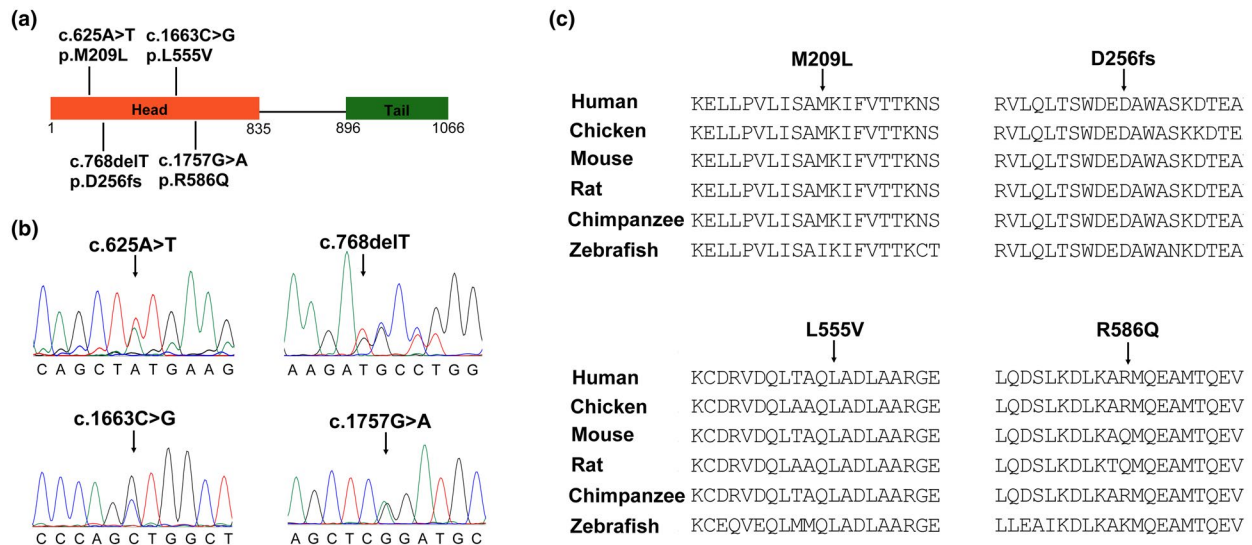


FIGURE 1 *VCL* variants identified in human NTD cases. (a) A schematic diagram showing the location of *VCL* variations identified in our NTD cohorts. (b) The electropherograms of the Sanger sequencing of four heterozygous variants in human NTD samples. (c) A partial alignment of the conserved amino acid sequences of *VCL* proteins from different vertebrates.

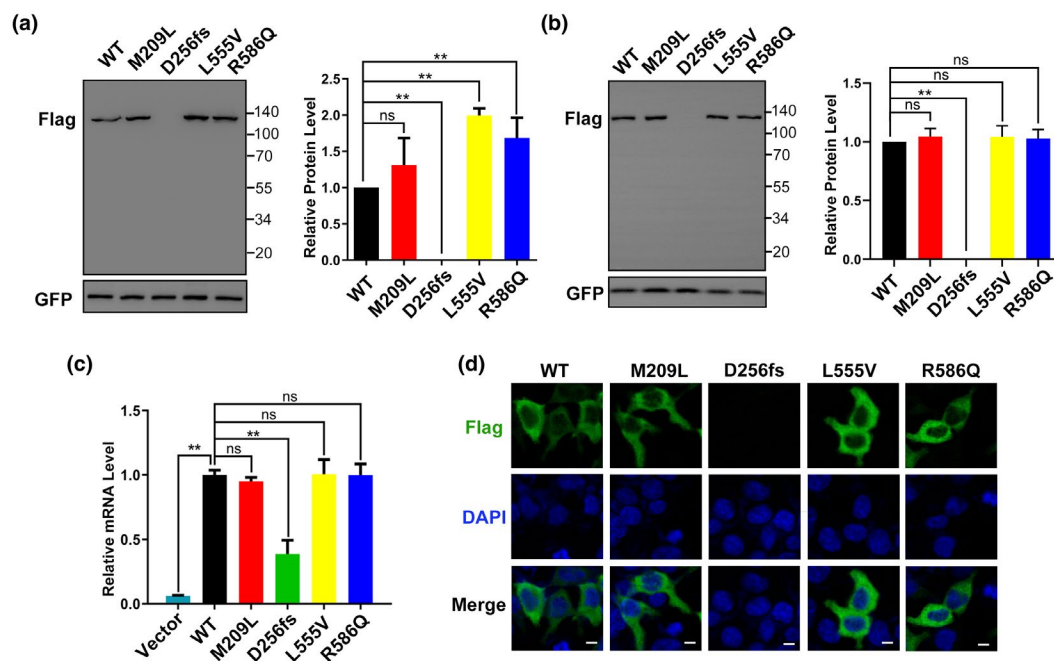


FIGURE 2 The expression and subcellular localization of *VCL* variants. (a and b) The representative image of Western blot and their quantification analysis of the exogenous wide-type and variant *VCL* proteins as indicated in HEK293T cells without (a) or with MG132 treatment (b). GFP co-transfected was used as a transfection control. (c) Statistical analysis of qRT-PCR of exogenous wide-type or variant *VCL* mRNAs in HEK293T cells. *GAPDH* was used as an internal control. (d) The representative fluorescent microscopic images of HEK293T cells transfected with Flag-tagged WT or variant *VCL* as indicates and immunoblotted with anti-Flag (green) and DAPI (blue), Scale bar: 20 μ m. Data were presented as mean \pm SD (N = 3). ***p* < 0.01, ns: not significant.

et al., 2018; Xu et al., 1998), the specific role of *VCL* in neural tube closure is not clear. Next, we checked the roles of wide-type *VCL* and NTD-specific *VCL* variants in cell migration by wound healing assay, a primary model widely used in cell movement-related morphogenesis (Xu et al., 1998). Our

results showed that wide-type *VCL* evidently inhibited cell migration, which was consistent with previous reports that loss of *VCL* led to increased cell migration (Chinthalapudi et al., 2014; Lausecker et al., 2018; Xu et al., 1998). Compared with wide type, p.L555V variant significantly restrained cell

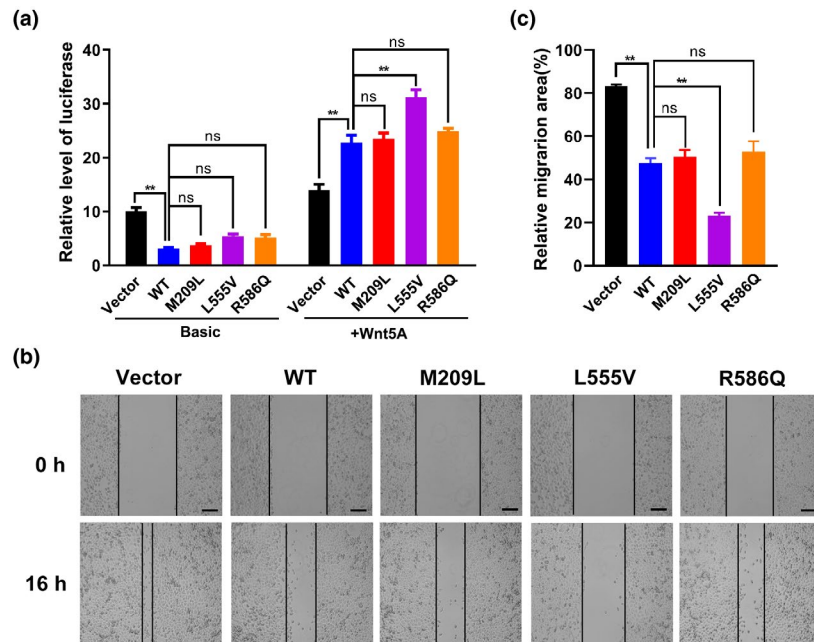


FIGURE 3 Effects of VCL variants on the PCP pathway and cell migration. (a) The statistical analyses of luciferase reporter assay for HEK293T cells co-transfected with expressing plasmids as indicated and planar cell polarity (PCP) reporter plasmids. Firefly luciferase activities were normalized by Renilla luciferase control. (b) The representative microscopic images of H1299 cells transfected with expressing plasmids as indicated and then subjected for wound healing assay at the indicated time. Scale bar: 300 μ m. (c) Quantification analysis of three independent wound healing experiments. Data were presented as mean \pm SD (N = 3). ** p < 0.01, ns: not significant.

migration with a gain-of-function effect (Figure 3b,c), while p.M209L and p.R586Q variants showed no distinct change in cell migration.

4 | DISCUSSION

To the best of our knowledge, this is the first study to demonstrate that VCL variants may contribute to the human neural tube defect. Here, four VCL variants (p.M209L, p.D256fs, p.L555V, p.R586Q) were identified as case-specific in a Chinese NTD cohort. VCL p.L555V variants, with elevated protein level, potentiated the Wnt5A-activated PCP signaling and more effectively inhibited cell migration, compared with the wide type, which suggests p.L555V is a gain-of-function variant. (Figures 2a and 3a-c). VCL p.M209L was assumed likely being a neutral variant with no change in the protein expression and functional study (Figures 2a,d and 3a,b). VCL p.R586Q variant performed similarly as wild type VCL in functional analysis although its protein level was significantly higher than wild VCL (Figures 2a and 3a,b). VCL p.D256fs variant did not express any detectable protein (Figure 2a and d), demonstrating it is a loss-of-function variant.

The diverse signaling pathways regulating cytoskeleton remodeling are coordinated by FAs and adhesion junctions. As a key component, VCL is indispensable for cytoskeleton remodeling and interacts with many partners such as F-actin,

Catenins, Talin, and PIP₂ (Dedden et al., 2019; Huang et al., 2017). Although it has been reported that VCL affected polarity (Carisey et al., 2013; Carvalho et al., 2019), whether VCL affects PCP signaling remains elusive. In the present study, we have demonstrated that VCL suppresses basic PCP signaling and stimulates the Wnt5A-activated PCP pathway (Figure 3a). Considering that PCP core modules, including FZDs, Vangls, Celsrs, DVLS, Prickle, and Diego, localize in adhesion junctions (Nikolopoulou et al., 2017), here we speculate that scaffold VCL may participate in the regulation of these functional PCP proteins in adhesion junctions. In addition, PCP signaling is a dosage-sensitive pathway and could be destructed by either decreased or increased signaling in *Xenopus*, zebrafish, and vertebrates (Roszko et al., 2009; Wallingford, 2005). Both loss-of-function and gain-of-function mutations in PCP core genes have been discovered in humans (Qiao et al., 2016; Robinson et al., 2012), so it is acceptable both loss-of-function and gain-of-function variants in VCL were potentially pathogenic since they altered PCP signaling balance.

Although *vcl* null mice displayed NTD and died at early gestation, while heterozygous mice appeared normal (Xu et al., 1998). In fact, our patient or fetuses diagnosed with NTDs harbored heterozygous variants. Considering multi-factor threshold model of NTDs and digenic heterozygous mutations of PCP signaling in mouse are responsible for NTDs (Greene et al., 2009), the two variants (p.D256fs and p.L555V) might co-operate with other mutations or modifiers

in signaling pathways or biological processes, to facilitate NTD pathogenesis.

In conclusion, here we identified four rare case-specific *VCL* variants from a Chinese NTD cohort and initially disclosed that both loss-of-function and gain-of-function variants of *VCL* may contribute to human neural tube defects.

5 | DATA AVAILABLE STATEMENT

Data available on request from the authors.

ACKNOWLEDGMENTS

We sincerely thank all of the subjects participated in this study.

CONFLICT OF INTEREST

The authors declare no conflict of interest.

AUTHORS' CONTRIBUTIONS

Y.W., Y.Q., and H.W. conceived the experiments. Y.W., Y.Q., and R.P. performed the experiments. Y.W. and Y.Q. analyzed the data. Y.W., Y.Q., and H.W. wrote the manuscript.

Funding information

Supported by grants from the National Key Research and Development Program of China (2016YFC1000502) and National Natural Science Foundation of China (31771669).

ORCID

Yalan Wang  <https://orcid.org/0000-0002-7538-3515>

REFERENCES

- Atherton, P., Stutchbury, B., Wang, D.-Y., Jethwa, D., Tsang, R., Meiler-Rodriguez, E., Wang, P., Bate, N., Zent, R., Barsukov, I. L., Goult, B. T., Critchley, D. R., & Ballestrin, C. (2015). Vinculin controls talin engagement with the actomyosin machinery. *Nature Communications*, 6, 10038. <https://doi.org/10.1038/ncomms10038>
- Au, K. S., Ashley-Koch, A., & Northrup, H. (2010). Epidemiologic and genetic aspects of spina bifida and other neural tube defects. *Dev Disabil Res Rev*, 16(1), 6–15. <https://doi.org/10.1002/ddr.93>
- Carisey, A., Tsang, R., Greiner, A. M., Nijenhuis, N., Heath, N., Nazgiewicz, A., Kemkemer, R., Derby, B., Spatz, J., & Ballestrin, C. (2013). Vinculin regulates the recruitment and release of core focal adhesion proteins in a force-dependent manner. *Current Biology*, 23(4), 271–281. <https://doi.org/10.1016/j.cub.2013.01.009>
- Carvalho, J. R., Fortunato, I. C., Fonseca, C. G., Pezzarossa, A., Barbacena, P., Dominguez-Cejudo, M. A., Vasconcelos, F. F., Santos, N. C., Carvalho, F. A., & Franco, C. A. (2019). Non-canonical Wnt signaling regulates junctional mechanocoupling during angiogenic collective cell migration. *Elife*, 8, e45853. <https://doi.org/10.7554/eLife.45853>
- Case, L. B., Baird, M. A., Shtengel, G., Campbell, S. L., Hess, H. F., Davidson, M. W., & Waterman, C. M. (2015). Molecular mechanism of vinculin activation and nanoscale spatial organization in focal adhesions. *Nature Cell Biology*, 17(7), 880–892. <https://doi.org/10.1038/ncb3180>
- Chinthalapudi, K., Rangarajan, E. S., Patil, D. N., George, E. M., Brown, D. T., & Izard, T. (2014). Lipid binding promotes oligomerization and focal adhesion activity of vinculin. *Journal of Cell Biology*, 207(5), 643–656. <https://doi.org/10.1083/jcb.201404128>
- Copp, A. J., Stanier, P., & Greene, N. D. (2013). Neural tube defects: recent advances, unsolved questions, and controversies. *The Lancet Neurology*, 12(8), 799–810. [https://doi.org/10.1016/S1474-4422\(13\)70110-8](https://doi.org/10.1016/S1474-4422(13)70110-8)
- De Marco, P., Merello, E., Consales, A., Piatelli, G., Cama, A., Kibar, Z., & Capra, V. (2013). Genetic analysis of disheveled 2 and disheveled 3 in human neural tube defects. *Journal of Molecular Neuroscience*, 49(3), 582–588. <https://doi.org/10.1007/s12031-012-9871-9>
- De Marco, P., Merello, E., Rossi, A., Piatelli, G., Cama, A., Kibar, Z., & Capra, V. (2012). FZD6 is a Novel Gene for Human Neural Tube Defects. *Human Mutation*, 33(2), 384–390. <https://doi.org/10.1002/humu.21643>
- Dedden, D., Schumacher, S., Kelley, C. F., Zacharias, M., Biertumpfel, C., Fassler, R., & Mizuno, N. (2019). The Architecture of Talin1 Reveals an Autoinhibition Mechanism. *Cell*, 179(1), 120–131 e113. <https://doi.org/10.1016/j.cell.2019.08.034>
- Greene, N. D., & Copp, A. J. (2014). Neural tube defects. *Annual Review of Neuroscience*, 37, 221–242. <https://doi.org/10.1146/annurev-neuro-062012-170354>
- Greene, N. D., Stanier, P., & Copp, A. J. (2009). Genetics of human neural tube defects. *Human Molecular Genetics*, 18(R2), R113–129. <https://doi.org/10.1093/hmg/ddp347>
- Harris, M. J., & Juriloff, D. M. (2010). An update to the list of mouse mutants with neural tube closure defects and advances toward a complete genetic perspective of neural tube closure. *Birth Defects Res A Clin Mol Teratol*, 88(8), 653–669. <https://doi.org/10.1002/bdra.20676>
- Huang, D. L., Bax, N. A., Buckley, C. D., Weis, W. I., & Dunn, A. R. (2017). Vinculin forms a directionally asymmetric catch bond with F-actin. *Science*, 357(6352), 703–706. <https://doi.org/10.1126/science.aan2556>
- Jm, L., & As, Y. (2013). Vinculin, cadherin mechanotransduction and homeostasis of cell-cell junctions. *Protoplasma*, 250(4), 817–829. <https://doi.org/10.1007/s00709-012-0475-6>
- Kibar, Z., Torban, E., McDearmid, J. R., Reynolds, A., Berghout, J., Mathieu, M., & Hayes, J. M. (2007). Mutations in *VANGL1* associated with neural-tube defects. *New England Journal of Medicine*, 356(14), 1432–1437. <https://doi.org/10.1056/NEJMoa060651>
- Lausecker, F., Tian, X., Inoue, K., Wang, Z., Pedigo, C. E., Hassan, H., Liu, C., Zimmer, M., Jinno, S., Huckle, A. L., Hamidi, H., Ross, R. S., Zent, R., Ballestrin, C., Lennon, R., & Ishibe, S. (2018). Vinculin is required to maintain glomerular barrier integrity. *Kidney International*, 93(3), 643–655. <https://doi.org/10.1016/j.kint.2017.09.021>
- Leck, I. (1974). Causation of Neural Tube Defects - Clues from Epidemiology. *British Medical Bulletin*, 30(2), 158–163. <https://doi.org/10.1093/oxfordjournals.bmb.a071187>
- Lei, Y., Fathe, K., McCartney, D., Zhu, H., Yang, W., Ross, M. E., & Finnell, R. H. J. H. M. (2015). Rare *LRP6* variants identified in spina bifida patients. *Human Mutation*, 36(3), 342–349. <https://doi.org/10.1002/humu.22750>
- Lei, Y., Zhang, T., Li, H., Wu, B., Jin, L., & Wang, H. (2010). *VANGL2* mutations in human cranial neural-tube defects. *New England Journal of Medicine*, 362(23), 2232–2235. <https://doi.org/10.1056/NEJMc0910820>

- Lei, Y., Zhu, H., Duhon, C., Yang, W., Ross, M. E., Shaw, G. M., & Finnell, R. H. J. P. O. (2013). Mutations in planar cell polarity gene SCRIB are associated with spina bifida. *PLoS One*, *8*(7), e69262. <https://doi.org/10.1371/journal.pone.0069262>
- Morita, H., Kajiura-Kobayashi, H., Takagi, C., Yamamoto, T. S., Nonaka, S., & Ueno, N. J. D. (2012). Cell movements of the deep layer of non-neural ectoderm underlie complete neural tube closure in *Xenopus*. *Development*, *139*(8), 1417–1426. <https://doi.org/10.1242/dev.073239>
- Murdoch, J. N., & Copp, A. J. (2010). The Relationship between Sonic Hedgehog Signaling, Cilia, and Neural Tube Defects. *Birth Defects Research Part A-Clinical and Molecular Teratology*, *88*(8), 633–652. <https://doi.org/10.1002/bdra.20686>
- Murdoch, J. N., Damrau, C., Paudyal, A., Bogani, D., Wells, S., Greene, N. D. E., Stanier, P., & Copp, A. J. (2014). Genetic interactions between planar cell polarity genes cause diverse neural tube defects in mice. *Disease Models & Mechanisms*, *7*(10), 1153–1163. <https://doi.org/10.1242/dmm.016758>
- Nikolopoulou, E., Galea, G. L., Rolo, A., Greene, N. D., & Copp, A. J. (2017). Neural tube closure: cellular, molecular and biomechanical mechanisms. *Development*, *144*(4), 552–566. <https://doi.org/10.1242/dev.145904>
- Qiao, X., Liu, Y., Li, P., Chen, Z., Li, H., Yang, X., Finnell, R. H., Yang, Z., Zhang, T., Qiao, B., Zheng, Y., & Wang, H. (2016). Genetic analysis of rare coding mutations of CELSR1-3 in congenital heart and neural tube defects in Chinese people. *Clinical Science (Lond)*, *130*(24), 2329–2340. <https://doi.org/10.1042/CS20160686>
- Robinson, A., Escuin, S., Doudney, K., Vekemans, M., Stevenson, R. E., Greene, N. D., & Stanier, P. (2012). Mutations in the planar cell polarity genes CELSR1 and SCRIB are associated with the severe neural tube defect craniorachischisis. *Human Mutation*, *33*(2), 440–447. <https://doi.org/10.1002/humu.21662>
- Roszko, I., Sawada, A., & Solnica-Krezel, L. (2009). Regulation of convergence and extension movements during vertebrate gastrulation by the Wnt/PCP pathway. *Seminars in Cell & Developmental Biology*, *20*(8), 986–997. <https://doi.org/10.1016/j.semcdb.2009.09.004>
- Johnson, R. P., & Craig, S. W. (1995). F-actin binding site masked by the intramolecular association of vinculin head and tail domains. *Nature*, *373*(6511), 261–264. <https://doi.org/10.1038/373261a0>
- Vasile, V. C., Ommen, S. R., Edwards, W. D., & Ackerman, M. J. (2006). A missense mutation in a ubiquitously expressed protein, vinculin, confers susceptibility to hypertrophic cardiomyopathy. *Biochemical and Biophysical Research Communications*, *345*(3), 998–1003. <https://doi.org/10.1016/j.bbrc.2006.04.151>
- Vasile, V., Will, M., Ommen, S., Edwards, W., Olson, T., & Ackerman, M. (2006). Identification of a metavinculin missense mutation, R975W, associated with both hypertrophic and dilated cardiomyopathy. *Molecular Genetics and Metabolism*, *87*(2), 169–174. <https://doi.org/10.1016/j.ymgme.2005.08.006>
- Wallingford, J. B. (2005). Neural tube closure and neural tube defects: Studies in animal models reveal known knowns and known unknowns. *American Journal of Medical Genetics Part C-Seminars in Medical Genetics*, *135c*(1), 59–68. <https://doi.org/10.1002/ajmg.c.30054>
- Xu, W., Baribault, H., & Adamson, E. D. (1998). Vinculin knockout results in heart and brain defects during embryonic development. *Development*, *125*(2), 327–337.
- Ybot-Gonzalez, P., Cogram, P., Gerrelli, D., & Copp, A. J. (2002). Sonic hedgehog and the molecular regulation of mouse neural tube closure. *Development*, *129*(10), 2507–2517.
- Ybot-Gonzalez, P., Gaston-Massuet, C., Girdler, G., Klingensmith, J., Arkell, R., Greene, N. D. E., & Copp, A. J. (2007). Neural plate morphogenesis during mouse neurulation is regulated by antagonism of Bmp signalling. *Development*, *134*(17), 3203–3211. <https://doi.org/10.1242/dev.008177>

SUPPORTING INFORMATION

Additional Supporting Information may be found online in the Supporting Information section.

How to cite this article: Wang Y, Qin Y, Peng R, Wang H. Loss-of-function or gain-of-function variations in *VINCULIN* (*VCL*) are risk factors of human neural tube defects. *Mol Genet Genomic Med*. 2021;9:e1563. <https://doi.org/10.1002/mgg3.1563>